Chem

Article

Production of biorenewable, enantiopure (S)-3-hydroxy-γ-butyrolactone for pharmaceutical applications

Graphical abstract

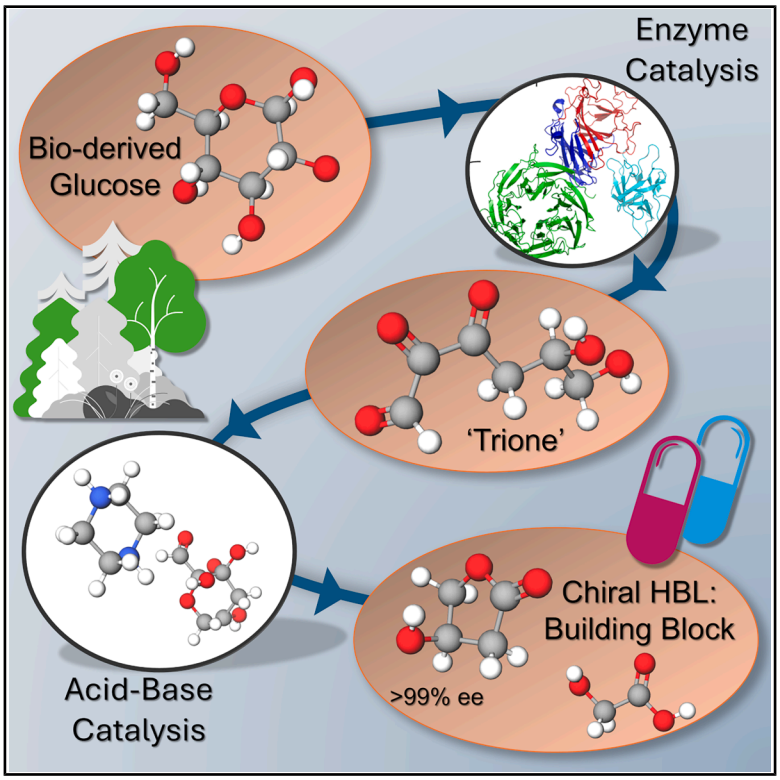

Highlights

- Enzymatic conversion of glucose to "trione," a highly labile chemical intermediate
- Production of (S)-3-hydroxy-γ-butyrolactone from "trione" using acid/base catalysis
- TEA suggests more than 60% cost reduction to produce (S)-3-hydroxy-γ-butyrolactone

Authors

Justin O.P. Waters, Elnaz Jamalzade, Hussein T. Abdulrazzaq, ..., James A. Dumesic, Philip J. Kersten, Thomas J. Schwartz

Correspondence

philip.j.kersten@usda.gov (P.J.K.), thomas.schwartz@maine.edu (T.J.S.)

In brief

Production of chiral building blocks is a significant cost driver in the manufacture of pharmaceuticals, which can be simplified by approaches that leverage both chemical and biological processes. A labile intermediate, "trione," can be produced from glucose using a modified aldos-2-ulose dehydratase enzyme, and the resulting trione is converted to (S)-3-hydroxy-γ-butyrolactone (HBL) using simple base catalysis. This ambient temperature, aqueous process is estimated to reduce the cost of HBL by more than 60%.

Waters et al., 2025, Chem *11*, 102665
December 11, 2025
https://doi.org/10.1016/j.chempr.2025.102665

CellPress

Please cite this article in press as: Waters et al., Production of biorenewable, enantiopure (S)-3-hydroxy-γ-butyrolactone for pharmaceutical applications, Chem (2025), https://doi.org/10.1016/j.chempr.2025.102665

Chem

CellPress

Article

Production of biorenewable, enantiopure (S)-3-hydroxy-γ-butyrolactone for pharmaceutical applications

Justin O.P. Waters,[1,2,6] Elnaz Jamalzade,[2,3,6] Hussein T. Abdulrazzaq,[1,2,6] Nathaniel Kuch,[4] Sampath R. Gunukula,[1,2] James A. Dumesic,[5] Philip J. Kersten,[4,*] and Thomas J. Schwartz[1,2,7,*]

[1]Department of Chemical and Biomedical Engineering, University of Maine, Orono, ME 04469, USA
[2]Forest Bioproducts Research Institute, University of Maine, Orono, ME 04469, USA
[3]Department of Chemistry, University of Maine, Orono, ME 04469, USA
[4]Forest Products Laboratory, USDA Forest Service, Madison, WI 53726, USA
[5]Department of Chemical and Biological Engineering, University of Wisconsin-Madison, Madison, WI 53076, USA
[6]These authors contributed equally
[7]Lead contact
*Correspondence: philip.j.kersten@usda.gov (P.J.K.), thomas.schwartz@maine.edu (T.J.S.)
https://doi.org/10.1016/j.chempr.2025.102665

THE BIGGER PICTURE The high price of pharmaceuticals is driven, in part, by the cost of materials and production. Some of the most expensive drugs contain chiral centers that are introduced during synthesis using a small number of chemical building blocks. These building blocks are both costly to produce and can lead to significant greenhouse gas emissions, both due to difficult recovery from low-concentration mixtures of chemical species and challenging reaction pathways. This work reports on a new approach for synthesizing pharmaceutical precursors that allows for the production of chiral species at high concentrations and yields, in water, and at room temperature. The reaction pathway starts with renewable glucose that is chemically pruned using biological catalysis to produce a highly reactive intermediate that is then converted by acid/base catalysis to the key chiral building block used to make statin drugs, (S)-3-hydroxy-γ-butyrolactone (HBL). This pathway reduces the cost of HBL by more than 60% relative to the state of the art that uses non-renewable, petroleum-derived feedstocks.

SUMMARY

Many pharmaceuticals include chiral centers, which are introduced using high-cost building blocks such as (S)-3-hydroxy-γ-butyrolactone, (S)-HBL. This species is used in the synthesis of many important drugs, including statins, antibiotics, and HIV inhibitors, and it is currently produced from fossil resources via a high-cost, high-emission process. Here, we show that a nearly quantitative yield of enantiopure (S)-HBL can be obtained from glucose at ambient temperature, using a combination of biological and chemical catalysis. Whole-cell enzyme catalysis converts glucose to a labile intermediate (denoted as trione) that is subsequently reacted to (S)-HBL by metal-free homogeneous acid/base catalysis. These reactions do not involve the C5 of glucose, leading to enantiopure (S)-HBL, produced at less than half the present cost. This approach can also be used to produce other commercially important building blocks from sustainable feedstocks: the enzymes used for trione production are active in converting xylose, leading to the acrylate co-monomer 3-hydroxypropionic acid.

INTRODUCTION

Americans spend ca. 550 billion USD on pharmaceuticals each year,[1] with some individuals paying upward of 10,000 USD each month.[2] Rising drug costs are in part driven by materials and production,[3] among the costliest of which are those that introduce chirality.[4] As such, only a handful of chiral species are used to produce a wide range of important pharmaceuticals.[5] An example of this category is (S)-3-hydroxy-γ-butyrolactone (HBL), used for synthesis of a range of drugs that are critical to public health, including cholesterol-lowering drugs (e.g., Lipitor and Crestor), antibiotics (e.g., Linezolid and Ezetimibe), HIV inhibitors, and nutritional supplements.[6,7] Moreover, both HBL and the related 2,3-dihydroxybutyrate have been

Please cite this article in press as: Waters et al., Production of biorenewable, enantiopure (S)-3-hydroxy-γ-butyrolactone for pharmaceutical applications, Chem (2025), https://doi.org/10.1016/j.chempr.2025.102665

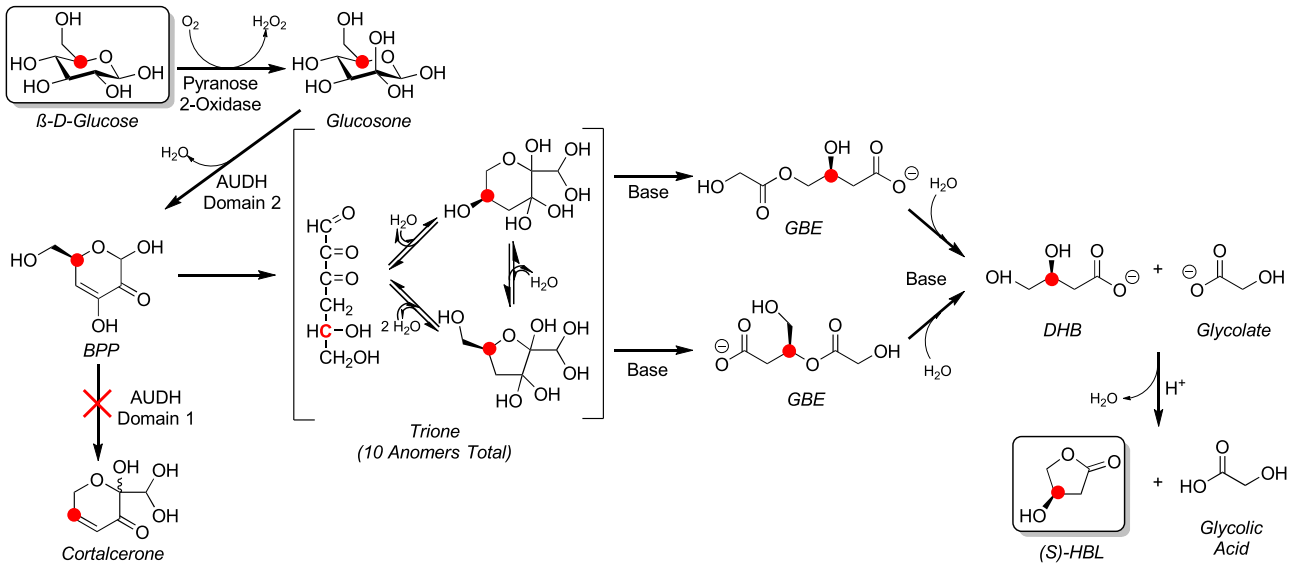

Figure 1. Enzymatic and catalytic route from glucose to (S)-3-hydroxy-γ-butyrolactone (HBL) and glycolic acid

Pyranose 2-oxidase converts glucose to glucosone, which is then converted to Basidiopyrone P (BPP, IUPAC name 4,5-dihydroxy-2-(hydroxymethyl)-2H-pyran-5-one) via domain 2 of Aldos-2-ulose dehydratase (AUDH). Domain 1 of AUDH is mutated to inhibit its function, leading to the formation of trione rather than cortalcerone. Trione undergoes a homogeneously base-catalyzed (e.g., with piperazine) retro-Aldol reaction to form an ester of 3,4-dihydroxybutyrate and glycolate (GBE). GBE can undergo base-catalyzed hydrolysis to yield glycolate and 3,4-dihydroxybutyrate (DHB), the latter of which forms HBL and GA upon acidification with HCl. Acid-catalyzed hydrolysis of GBE yields HBL and GA directly. Carbon 5 of glucose, highlighted in red, remains unaffected by any of the catalytic steps, leading to production of chiral (S)-HBL.

identified by the US Department of Energy as highly valuable precursors to a range of chemicals and plastics, regardless of chirality.[7] Nearly all commercially available HBL is currently derived from petroleum, with wholesale costs reported[8] in 2013 to be ca. 450 USD kg^{-1}, driven by a complex production pipeline that uses costly precious metals and purified enzymes as catalysts and which includes unit operations that require significant energy and produce significant emissions.[9]

Accordingly, there have been several attempts to produce HBL sustainably from renewable resources using low-cost methods. For example, naturally occurring L-malic acid can be converted to HBL by reduction, which Saito et al. performed using borane dimethyl sulfide and sodium borohydride, although the process requires air- and moisture-free conditions, and dimethyl sulfide is highly toxic.[10] Hollingsworth used lithium borohydride to perform the same reduction, using dimethyl malate as an intermediate, and while less hazardous than the use of borane dimethyl sulfide this process is limited by over-reduction to produce 1,2,4-trihydroxybutane in an undesired side reaction.[11] More recently, Dhamankar and coworkers used metabolic engineering with recombinant *E. coli* to produce (S)-HBL from D-glucose.[8,12] Their optimized cell line achieves 24% of the theoretical maximum yield of HBL and DHB, but at titers of only 0.3 g L^{-1} HBL and 0.7 g L^{-1} DHB. Similarly, Cao et al. used a different strain of recombinant *E. coli* to produce (S)-HBL from D-xylose, obtaining a titer of 3.5 g L^{-1} at 52% yield on xylose with 99.3% enantiomeric excess (ee).[13] Notably, these methods produce HBL at relatively low concentrations (less than 1 wt %), which is often not enantiomerically pure; thus, while the reaction-associated costs may decrease, recovery and purification will remain costly, ultimately limiting their practicality.

We have previously described the benefits of combining biological and chemical methods for producing biobased chemicals,[14,15] and we showed that the combination of whole-cell enzyme catalysis and heterogeneous acid catalysis can be uniquely effective, e.g., for the production of furylglycolic acid (a co-monomer for lactic acid) from glucose via cortalcerone as an intermediate.[16] Here, we build on this approach by modifying the enzymatic pathway to cortalcerone to instead produce a highly reactive intermediate we refer to as "trione" that can subsequently be converted to (S)-HBL via homogeneous acid/base catalysis. We produce HBL that is enantiomerically pure because none of the reactions involve the chiral C5 carbon of glucose, which exists natively in the correct orientation to produce (S)-HBL. An overview of the sequence of chemical transformations is shown in Figure 1.

RESULTS AND DISCUSSION

Trione synthesis from glucose

The synthetic route to trione is derived from the fungal metabolic pathway for the synthesis of the antibiotic cortalcerone from glucose, which involves only two enzymes, pyranose 2-oxidase (POX) and aldos-2-ulose dehydratase (AUDH).[17,18] POX oxidizes glucose to glucosone with oxygen or quinones as electron acceptors,[19–23] and glucosone is dehydrated and isomerized to cortalcerone by AUDH (Figure 1). The genes for POX and AUDH used in our studies are immediately adjacent to each other in the *Phanerochaete chrysosporium*

Please cite this article in press as: Waters et al., Production of biorenewable, enantiopure (S)-3-hydroxy-γ-butyrolactone for pharmaceutical applications, Chem (2025), https://doi.org/10.1016/j.chempr.2025.102665

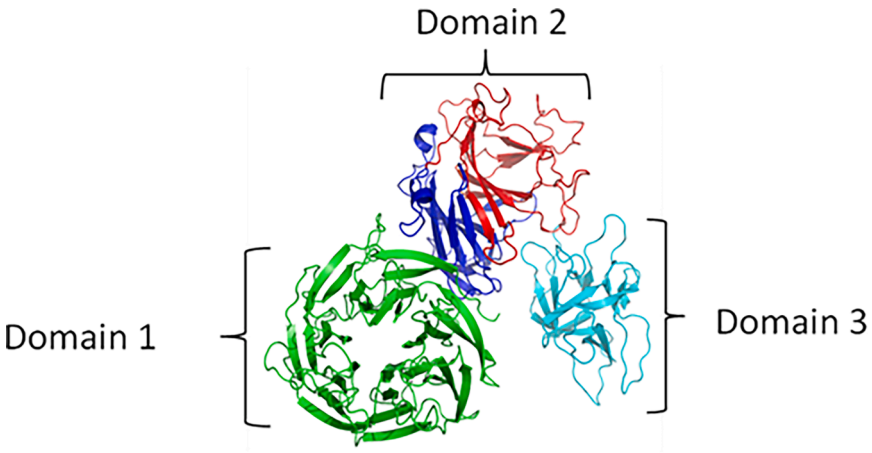

Figure 2. Structure of Aldos-2-ulose dehydratase (AUDH)

The enzyme is homo-dimeric and contains three domains, designated here at D_1, D_2, and D_3. Variants with mutations in the domain are indicated with an asterisk (e.g., $D_1{}^*D_2D_3$ has a mutation in domain 1 that we have found prevents conversion of glucosone to cortalcerone, instead producing trione).

genome (protein model 6207208 and 6207226 respectively, https://mycocosm.jgi.doe.gov/Phchr4_2/Phchr4_2.home.html), an organizational pattern also observed in other wood-decay fungi.[24] We previously described the synthesis of glucosone from glucose by *E. coli* whole cells with POX,[25] which we expand on here to demonstrate the synthesis of trione from glucosone by an AUDH variant that consumes glucosone but is unable to make cortalcerone.

The design of this AUDH variant is a result of our studies to deconvolute the catalytic roles for the domains of AUDH, the crystal structure of which is shown in Figure 2. The 900-amino-acid-long enzyme is homo-dimeric and has the following three domains: domain 1 (D_1) consisting of 433 amino acids (residues 1–433) folded into a seven-bladed β propeller, domain 2 (D_2) consisting of 306 amino acids (residues 434–739) with two β-sandwich structures characteristic of a cupin fold, and domain 3 (D_3) with 161 amino acids is a lectin domain (residues 740–900) and joined to D_2 by a short linker.[26] Crystal structure analysis of AUDH indicates substrate intermediate complexation with domains 1 and 2 at His155 and His641, respectively, suggesting that these domains are catalytically active, while domain 3 may have a role in carbohydrate binding.[26] To probe the function of D_1, we constructed a variant where histidine at position 155 was substituted with phenylalanine (His155Phe; $D_1{}^*D_2D_3$). Similarly, a His641Phe ($D_1D_2{}^*D_3$) variant was constructed to potentially inactivate domain 2. A variant containing only amino acids 1–433 (D_1) proved valuable to exclude any activity of domains 2 and 3 (Table S1). Recombinant expression in *E. coli* of all three variants produced soluble protein as determined by SDS-PAGE analyses.

The wild-type $D_1D_2D_3$ and its variants were studied in whole-cell reactions with 10% glucosone, with product analysis by NMR. As shown in Table S2, catalysis with wild-type $D_1D_2D_3$ provided cortalcerone, while $D_1{}^*D_2D_3$ produced trione. There was no reaction of $D_1D_2{}^*D_3$ with glucosone, but $D_1{}^*D_2D_3$ and $D_1D_2{}^*D_3$ complemented to produce cortalcerone. Likewise, the D_1 variant complemented $D_1{}^*D_2D_3$ to produce cortalcerone, while there was no activity with the D_1 variant alone. This series of reactions provided evidence that D_2 in $D_1{}^*D_2D_3$ catalyzes the initial dehydration of glucosone and that D_1 is responsible for a subsequent reaction. These results are contrary to previous literature based on crystal structure analysis alone, which suggested that D_1 is responsible for the initial dehydration of glucosone.[26]

Although the NMR evidence from whole-cell experiments indicated that D_2 of $D_1{}^*D_2D_3$ is responsible for the initial dehydration step of glucosone, the resulting product (i.e., trione) is not the expected initial product from glucosone dehydration. Instead, an initial UV-absorbing intermediate (λ_{max} = 265 nm) is reported with native AUDH, consistent with an initial dehydration across C3 and C4 of glucosone; this intermediate is chemically unstable and converts to a non-absorbing product.[18] We hypothesize that the trione produced by $D_1{}^*D_2D_3$ is this non-absorbing product. Accordingly, we analyzed AUDH-variant-catalyzed reactions of glucosone via *in situ* UV spectroscopy, where cell-free extract of AUDH was used to avoid UV absorption by the cells. Figure 3A shows wild-type AUDH leading to an initial accumulation at 265 nm followed by cortalcerone formation (characterized by UV absorption at 230 nm), consistent with the activity of native AUDH.[18] The $D_1{}^*D_2D_3$ variant was successful in halting D_1 activity and consequently showed only accumulation at 265 nm (Figure 3B). The D_1 variant without D_2 and D_3 showed no reaction (Figure 3C); however, a combination of both $D_1{}^*D_2D_3$ and D_1 re-establishes wild-type functionality with a similar initial build-up at 265 nm followed by cortalcerone formation.

On the basis of our results, we propose that the initial intermediate produced by domain 2 of $D_1{}^*D_2D_3$ has the structure in Figure 1, which we refer to by the trivial name **basidiopyrone P** (BPP; the IUPAC name is 4,5-dihydroxy-2-(hydroxymethyl)-2H-pyran-5-one), consistent with the tradition of naming pyrones produced by Ascomycetes as ascopyrones (e.g., ascopyrone M from *Microthecium*; ascopyrone P from *Pezizales*; ascopyrone T from *Tuberales*; here basidiopyrone P from *Phanerocheate*, a basidiomycete).[27,28] The BPP produced by $D_1{}^*D_2D_3$ is chemically unstable and follows a first-order decay with a half-life of 3.7 min in 0.1 M phosphate buffer (pH 6).

The structure of BPP is also suggested by the analogous AUDH-catalyzed conversion of anhydrofructose (AF) to microthecin (Figure S1), which involves an intermediate named ascopyrone M (APM) for which chemical structure information has been previously reported.[27,29] Our ability to produce BPP and trione independently from cortalcerone has also allowed us to clarify that trione is not a substrate intermediate for cortalcerone production but, rather, that BPP itself is directly converted to cortalcerone, catalyzed by D_1 of AUDH. The analogous set of

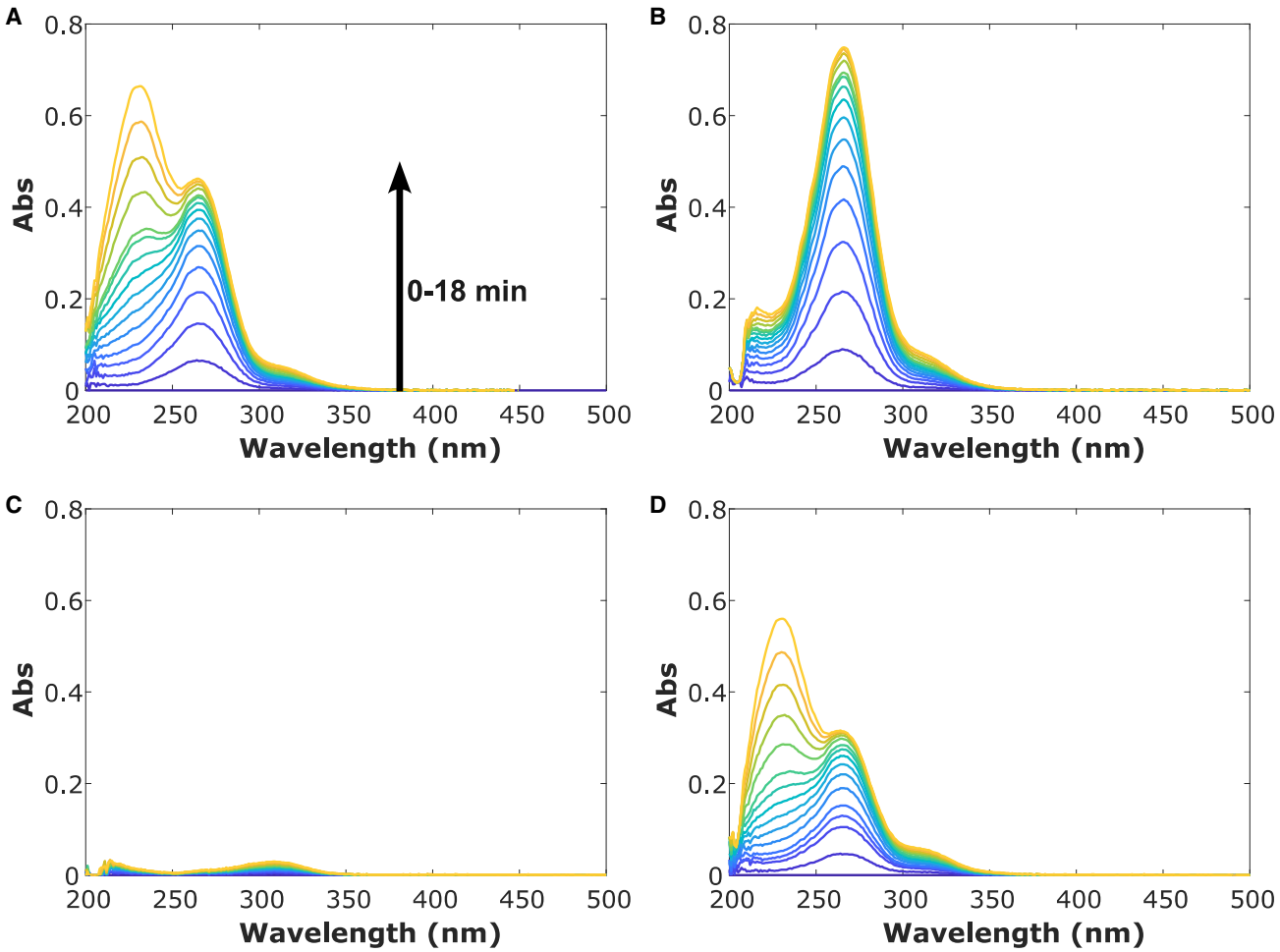

Figure 3. *In situ* UV spectroscopy of glucosone conversion using AUDH variants

(A) Wild-type $D_1D_2D_3$ initially produces BPP (λ_{max} = 265 nm) which is converted to cortalcerone (λ_{max} = 230 nm).

(B) The mutation to domain 1 in $D_1{}^*D_2D_3$ prevents the production of cortalcerone, leading to an accumulation at A_{265}.

(C) D_1 (domain 1 alone) has no activity on its own with glucosone.

(D) However, addition of D_1 to a reaction with $D_1{}^*D_2D_3$ re-establishes wild-type activity as seen with $D_1D_2D_3$. Collectively, these reactions indicate that catalysis is initiated by domain 2, and domain 1 then catalyzes the subsequent reaction to cortalcerone from an intermediate generated by domain 2.

reactions hold true for conversion of AF to microthecin via APM. Full details of these experiments are provided in the supplemental information.

Trione conversion to HBL

Having identified that trione can be produced intentionally from glucosone, we sought to demonstrate its use as a chemical intermediate for production of HBL. Trione was first obtained using whole cells containing the $D_1{}^*D_2D_3$ variant of AUDH. ^{13}C-NMR spectroscopy of the product solution from reaction of 555 mM glucosone was used to identify the products, which exist as an equilibrated distribution of 10 anomers (see Figure S8), with two hydrated and cyclized anomers being suitable for conversion to DHB via a retro-Aldol reaction (see Figure 1). To evaluate this possibility, a trione solution (0.156 M, diluted from the $D_1{}^*D_2D_3$-catalyzed reaction product) was treated with sodium bicarbonate (0.3 M, in trione solution) at 298 K, which converted the complex anomeric mixture into a glycolate ester of DHB (GBE), achieving 91 mol % yield in 23 h (entry 1 Table 1). Hydrolysis of this ester at 330 K with HCl yields DHB and glycolic acid (GA), with the DHB spontaneously lactonizing to produce HBL at low pH. The final yield of HBL based on glucose fed was 88 mol % based on high-performance liquid chromatography (HPLC) analysis of the final reaction product.

We next evaluated three other homogeneous base catalysts for their reactivity in forming GBE from trione at 298 K, with results shown in Table 1. The maximum GBE yield obtained over $NaHCO_3$ was 91 mol % (Figure S5). Bis-tris base ($C_8H_{19}NO_5$) achieved 98 mol % yield of GBE (Figure S6), with a slight increase in the turnover frequency (TOF, 0.07 vs. 0.05 h^{-1}). In contrast, the maximum yield of GBE over tris base ($C_4H_{11}NO_3$) was only 37% and ultimately decreased below 10% due to hydrolysis of GBE, ultimately forming DHB and GA (Figure S7). Piperazine ($C_4H_{10}N_2$) was the most reactive base examined,

Please cite this article in press as: Waters et al., Production of biorenewable, enantiopure (S)-3-hydroxy-γ-butyrolactone for pharmaceutical applications, Chem (2025), https://doi.org/10.1016/j.chempr.2025.102665

Table 1. Reactions of trione using several homogeneous base catalysts. All reactions performed at 298 K with 0.156 mol L^{-1} trione and 0.3 mol L^{-1} base. Product analysis was performed by NMR spectroscopy

Entry	Catalyst	Max. GBE yield (%)	DHB/GA yield[a] (%)	GBE yield (%)[a]	TOF(h^{-1})[b]	Base consumed (mol L^{-1})	PA (kJ mol^{-1})
1	$NaHCO_3$	91	0	91	0.05	0.065	920.3
2	Piperazine	23	>99	0	0.14	0.28	979.2
3	Tris base	37	14	0	0.06	0.298	972.4
4	Bis-tris base	98	0	96	0.07	0.11	928.1

[a]Measured at 23 h, trione conversion >99%. Yields in Table 1 reported on a per-mol basis relative to trione fed (i.e., mol GBE:mol trione).
[b]Turnover frequency measured for GBE production normalized to base concentration at <15% conversion using 0.03 mol L^{-1} base.

with a TOF 2–3 times greater than the other catalysts. The significant increase in rate is evident when comparing the GBE yield in Figure 4A, where the highest measured yield of GBE obtained over piperazine was only 23% (at the shortest time point where data could be collected). Notably, the increase in rate also translates to an increase in the rate of GBE hydrolysis, and catalysis with piperazine ultimately led to >99 mol % yield of DHB and GA at long times (Figure 4A). Because these reactions are carried out at high pH, when GBE is hydrolyzed to DHB and GA, these species are produced as piperazine or tris salts with a corresponding decrease in the concentration of base at the completion of the reaction.

We monitored the reaction using *operando* ^{1}H NMR spectroscopy, where the improved sensitivity relative to ^{13}C NMR allows for shorter data collection intervals, although the spectra are more challenging to interpret due to overlapping shifts. Using a combination of ^{1}H-NMR, DEPT-135-^{13}C-NMR, and heteronuclear single quantum coherence (HSQC) experiments (see Figures S9–S11), we identified the presence of DHB, HBL, and both GBE isomers shown in Figure 1, as well as several polyol species formed in small quantities during the trione ring-opening reaction. Figure 4B shows spectra collected over 12 h, with trione (marked by the shifts centered around 1.8 ppm) consumed rapidly during the first 7 min of reaction. After 16 min of reaction, resonances appear around 2.7 and 4.2 ppm, which are assigned to GBE, after which they decrease slowly in intensity concomitant with appearance of shifts at 2.2 and 3.6 ppm that correspond to DHB. Concentrations extracted from these spectra are plotted with respect to reaction time in the inset of Figure 4A, a fit of which confirms that GBE is an intermediate in the conversion of trione into DHB and GA, consistent with the reaction network shown in Figure 1. The isomer of GBE formed from the pyranose form of trione (top path in Figure 1) was more prominent, likely due to greater stability of the pyranose form of trione, similar to glucosone.[19]

The rate at which trione is converted to GBE, and the extent of sequential hydrolysis to form DHB, varies with the identity of the base catalyst. A retro-Aldol reaction requires a carbonium ion transition state bound to the base catalyst, which suggests that the rate of C-C bond scission should scale with the strength of the base. Base strength can be described by the proton affinity (PA),[30] which was calculated using ground state density functional theory (DFT) with Gaussian 16 software.[31] The PA quantitatively describes the basicity of a molecule as the enthalpy difference between the neutral molecule and its protonated analog, which is equivalent to the negative of the gas-phase deprotonation energy (DPE) commonly used in quantifying the strength of Brønsted acids. The enthalpy is reaction and location dependent, meaning that it is influenced by the combination of reactants and the space occupied by the protons on a given acceptor. The PA was thus estimated as the difference between the total enthalpies of the protonated and neutral form of the homogeneous bases. The log of the TOF scales linearly with the

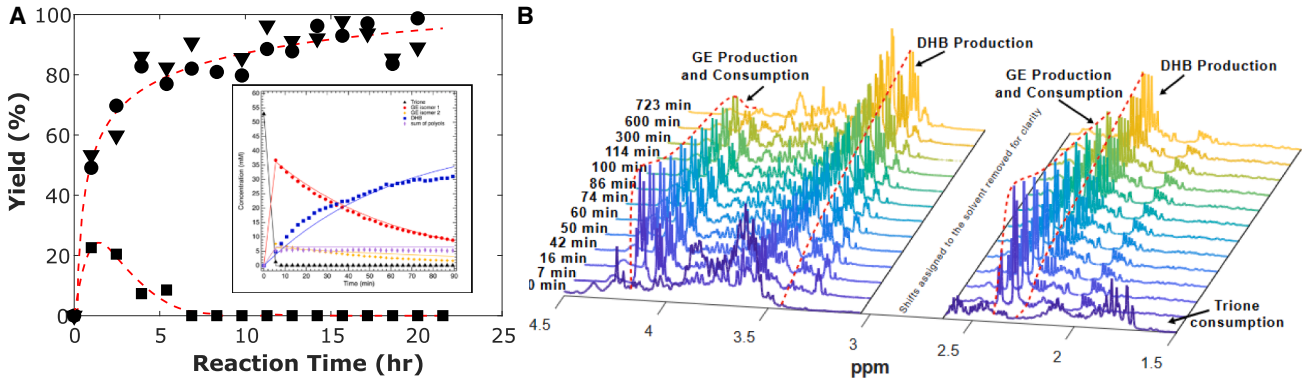

Figure 4. Reactions of trione using piperazine as a catalyst

(A and B) (A) GBE (■), GA (▾), and DHB (●) yields as a function of reaction time using 0.3 mol/L piperazine as a catalyst with 0.156 mol/L trione at 100% conversion. Inset: concentrations extracted from ^{1}H-NMR spectra at short times showing rapid consumption of trione and early production of GBE. (B) ^{1}H-NMR spectra collected during short reaction times using 0.05 mol/L trione and 0.15 mol/L piperazine. All reactions performed at 298 K in aqueous solvent

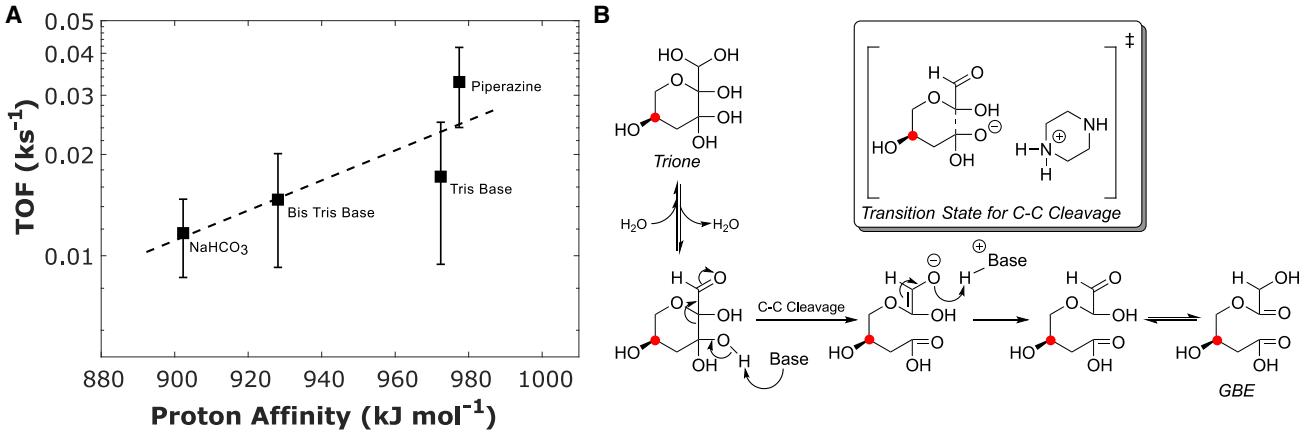

Figure 5. Proposed mechanism for trione conversion to GBE

(A) The log of the TOF for GBE production is a linear function of the PA of the four bases studied here. All reactions were performed at 298 K in aqueous solvent with 0.156 mol/L trione and 0.03 mol/L base. TOFs were measured below 15% conversion and are normalized to the base concentration. Error bars correspond to 95% confidence intervals.

(B) Proposed retro-Aldol reaction sequence by which trione is converted to GBE over homogenous base catalysts. Highlighted in the box is the proposed transition state for C-C bond cleavage with piperazine as a catalyst, where the dashed bond is being cleaved.

resulting PA values, as shown in Figure 5A, suggesting the activation energy for the reaction is modified by the PA and confirming the involvement of a carbonium ion transition state in the rate-controlling step, which would be consistent with the mechanism shown in Figure 5B.

Production of DHB in the presence of piperazine results in formation of the piperazine salt of DHB (*vide supra*), but acidification of the reaction solution results in conversion of the DHB salt into the corresponding lactone (i.e., HBL) at low pH.[32,33] Thus, we added sufficient hydrochloric acid to reduce the pH of the product solution to 0.7, the optimum level reported in literature.[8,12] A maximum yield of 88 mol % HBL (quantified by HPLC analysis) was obtained when the acidification was carried out at 330 K, resulting in an HPLC-quantified HBL titer of 14 g L^{-1} using 0.156 M trione solution (Figure S12), nearly an order of magnitude higher than the best titer obtained using biocatalysis alone.[13] Because we do not observe any products that would be indicative of HBL dehydration or other degradation,[34] it is likely that the yield is limited by equilibrium, rather than due to side reactions, which would allow for nearly quantitative production of HBL at commercial scale, with appropriate process design.

The highest value application of HBL is as a pharmaceutical precursor, which depends on its enantiomeric purity. Because none of the reactions shown in Figure 1 modify the C5 carbon of glucose, we expected the HBL to exist purely in the (S) form. To verify the enantiomeric purity, we used a Supelco™ β-Dex 225 capillary GC column, which has previously been used to evaluate the enantiomeric purity of HBL.[35] Following the same procedure, we observed only (S)-HBL and not (R)-HBL, indicating an enantiomeric excess of >99% (Figure S13). Quantification of the enantiomers was performed using GC-FID following extraction of HBL from the aqueous phase into ethyl acetate, confirming the HBL yield of 88% earlier estimated by HPLC and ^{1}H-NMR. Notably, liquid-liquid extraction can also be used to recover HBL from the aqueous phase at scale, so we measured the partition coefficient for HBL extraction in ethyl acetate, tetrahydrofuran (THF), and propylene carbonate (Figure S14). The highest partition coefficient was 1.3 ± 0.5 using THF as an extraction solvent.

Economic assessment of HBL production

A techno-economic analysis (TEA) was conducted to determine the economic viability of the process described here, using the discounted cash flow method with an assumed 10% internal rate of return.[36] An annual production capacity of 120 tonnes of HBL was selected based on market demand.[37] The HBL production process (Figure S15) consists of (1) POX and AUDH cell synthesis, (2) high purity oxygen production, (3) conversion of glucose to glucosone using POX cells, (4) conversion of glucosone to trione using AUDH cells, (5) upgrading trione to DHB using piperazine, (6) acidification of DHB to HBL using HCl, and (7) separation and purification of HBL. Hanging bag reactors (developed by Leidos) were chosen for catalysis using POX cells and AUDH cells. Continuous stirred tank reactors were chosen for the formation of DHB and GA from trione and for the subsequent acidification of DHB to produce HBL. The product stream consists of HBL, GA, water, piperazine chloride, and residual buffer salts, and is sent to two liquid-liquid extraction columns, where the HBL is extracted into ethyl acetate. Finally, distillation and vacuum evaporation are employed to recover ethyl acetate and produce HBL at a purity higher than 99.9%. In this configuration, the GA remains in the wastewater along with other impurities, although in practice, it would be advantageous to recover and purify GA for sale as a co-product.

ASPEN plus software was used to size process equipment for the separation and purification train, continuous stirred tank reactor, and the compressor.[38] The remaining units were sized using rules of thumb (seed trains and centrifuge), vendor data (hanging bag reactors), and published simulation data

(PSA).[39–41] The process equipment size was selected as a basis to assess the installed equipment costs (Table S3), which were then updated to 2022 dollars using chemical engineering cost indices. Finally, the cost factors developed by the National Renewable Energy Laboratory (NREL) as a function of the total installed equipment cost were used to determine the additional costs, such as site development and project contingency, associated with the total capital investment. The material and energy balances were used to calculate the operating costs.[36] The capital and the annual operating costs to produce HBL at the selected scale were determined to be 32.6 MM USD and 15.6 MM USD, respectively (Tables S4 and S5). Approximately 40% of the operating costs are attributed to the cost of piperazine. At this scale, the TEA predicts a minimum selling price of HBL of 162 USD/kg, which is 64% lower than the 450 USD/kg reported as the current state of the art.[8]

OUTLOOK

The new pathway reported in this paper for producing enantiomerically pure HBL is not only more sustainable than existing methods (e.g., using biomass feedstocks, mild temperatures, and aqueous solvent), but it is also more economically favorable. Moreover, while not explored in depth in our economic analysis, our method yields biobased GA as a byproduct, a chemical of increasing importance that has spurred research interest in its synthesis from biomass sugars.[42] Commercial GA is generally delivered as a technical grade,[43] in aqueous solvent, and so sale as a co-product would require little additional investment beyond what is outlined above for HBL. In contrast, metabolic engineering approaches have been used to produce glycolate from glucose,[44] although such methods rely on monocultured, engineered organisms, are generally not tolerant of feedstock impurities, and require expensive preprocessing of real biomass feeds.[45]

The combination of biological and chemical catalysis presented here for synthesis of HBL provides advantages not realized by using metabolic-pathway engineering or chemical catalysis alone. Instead of catalyzing a biological pathway from glucose to HBL, we show a simpler pathway from glucose to trione, requiring only two biocatalysts and producing a small, neutral product, i.e., trione. This approach allows a two-step process using whole cells where membrane permeability is not an issue and cell viability is not required. This approach also circumvents the need for fed-batch cultures (used elsewhere to prevent toxic conditions), co-feedstock additions (to compensate for metabolic deficiencies), and pH control (to neutralize organic acid products).[12,44,46] Furthermore, the steps for the synthesis of trione can be optimized individually for best characteristics and for high expression. An important enabling discovery for this approach is the synthesis of new enzymes with homology to D_2 that can replace D_1*D_2D_3 in the synthesis of trione by whole-cell catalysis. Similarly, trione is an attractive chemical intermediate due to its diverse chemical functionality and labile reactivity, thereby avoiding the selectivity challenges and resulting hazardous conditions that have plagued HBL synthesis from L-malic acid and enabling the use of simple and inexpensive homogeneous acid/base catalysts.

Finally, the approach presented here for synthesis of HBL can be extended to other chemical systems. For example, D-xylose is also a substrate for POX[18] for production of xylosone, which in turn is a substrate for AUDH[18] and could be used to produce xylo-trione. Analogous chemical upgrading of xylo-trione would provide 3-hydroxy propionic acid (HPA) and GA. HPA is one of the biobased platform chemicals identified by DOE with greatest potential for commercial applications, as is HBL, regardless of chirality.[7,47] The economic viability for HPA from xylose would likely not be as favorable as (S)-HBL from glucose because xylose is a poorer substrate than glucose for POX,[48] and the price of HPA is lower than chiral (S)-HBL. The similarities in processing could ultimately lead to synergistic co-production of HPA, GA, and (S)-HBL all from a single biorefinery.

METHODS

Bacterial strains and plasmids

The cDNA sequence (GenBank accession number AY522922) encoding POX of *P. chrysosporium* BKM-F-1767 (ATCC 24725),[19] with an N-terminal T7-tag and a C-terminal His6 tag,[48] was synthesized for optimized expression in *E. coli*, inserted in pJ414 (ATUM, Newark, CA, USA) and transformed into BL21(DE3).[25] The cDNA sequence (GenBank accession number KF699142) encoding AUDH from *P. chrysosporium* RP78, a homokaryotic strain derived from BKM-F-1767, was synthesized with a C-terminal His6 tag for optimized expression in *E. coli*, inserted in pJ414 (ATUM, Newark, CA, USA) and transformed into BL21(DE3).[16] This wild-type AUDH with C-terminal tag is designated $D_1D_2D_3$ (see Table S1). The AUDH variants are based on $D_1D_2D_3$ sequence with amino acid substitutions and deletions achieved by DNA synthesis (ATUM, Newark, CA, USA). All constructs are transformed in *E. coli* BL21(DE3).

Protein modeling

The PyMol model for AUDH is based on PDB entry 4A7K[26] using cDNA sequence (GenBank accession number KF699142) encoding AUDH from *P. chrysosporium* RP78, a homokaryotic strain derived from BKM-F-1767.[16] This 900-amino-acid sequence differs at 4 positions from the AUDH of *P. chrysosporium* ATCC 32629 on which the PDB entry is based.[26]

Growth and preparation of cells for catalysis

E. coli cells for all studies reported here (e.g., in glucosone synthesis, trione synthesis, and AUDH variant characterizations) were prepared in the same manner and similar to what we reported previously.[25] Auto-induction medium[49] with modifications[50] were used. Briefly, each liter of auto-induction medium contains 48 g terrific broth (TB) powder, 2 mM $MgSO_4$, 0.2× trace metals (1,000× trace metals, Teknova Cat. No: T1001), 28 mM di-sodium succinate, 0.005% antifoam 204, 8 g glycerol, 0.15 g glucose, and 5 g lactose. Carbenicillin (100 μg ml^{-1} final) provides selection. 500 mL of inoculated auto-induction medium in 2-L baffled flasks are incubated at 250 rpm, 20°C for 30 h. Cells are harvested as 40-mL aliquots in 50-mL conical centrifuge tubes at 4,000 × g for 15 min. The supernatants are removed, and the cell pellets overlaid with 10 mM citrate pH 6,

0.9% saline buffer to prevent freezer burn before storage at −20°C. Prior to use of the cells in catalysis, the frozen cells are thawed and washed twice (40 ml) in 0.9% saline, 10 mM citrate pH 6 buffer.

Synthesis of glucosone

Glucosone is prepared from 0.55M glucose (10% w/v) in 10 mM citrate pH 6 with washed whole cells (described earlier) in disposable pillow bioreactors.[25] Cells expressing POX from 40 mL of culture (about 2 g wet cells) are sufficient to catalyze a 200-mL reaction in 18 h.[25] Catalase from bovine liver (Sigma C40) at 10 mg/200 mL reaction provides protection from peroxide.

Synthesis of trione

Trione is prepared from 40 ml of 0.55M glucosone (adjustment to pH 6, as necessary) in a 50-mL conical centrifuge tube containing D_1*D_2D_3 washed cells (derived from 40 mL of culture, about 2 g wet weight cells) with mixing end-over-end (20 rpm) overnight (about 18 h). The trione solution is recovered by centrifugation and then sterilized by ultrafiltration (Steriflip, 0.22μm Millipore).

AUDH variant characterization with whole cells by NMR

Reactions used 1.5 mL of 0.55M glucosone in a 2-mL Eppendorf tube together with washed cell pellets (as described previously) derived from 1.5 mL of wild-type or AUDH variant cultures. Mixing was end-over-end (20 rpm) for approximately 18 h and the supernatant recovered for analysis after centrifugation. NMR instrumentation is as described previously.[25]

AUDH variant characterization with cell-free extract by UV spectroscopy

UV-spectroscopic analyses required a homogenous enzyme solution. Cells derived from 40 mL of culture (described earlier) are sonicated (Qsonica Model Q700) in 10 mL of sonication buffer (50 mM Tris pH 8, 50 mM NaCl, 5% glycerol), centrifuged and aliquots of 1.5 mL stored at −20°C. Spectroscopic activity was measured using a microplate reader (BioTek Epoch 2). Quartz cuvette scans were taken from 200–500 nm in 1 nm steps using the sweep read mode for a total read time of 15 s. Reactions were in 0.1 M phosphate buffer, pH 6 and contained 10 mM glucosone and 5 μL of sonicate to a final volume of 500 μL. Spectra were processed by subtracting the first spectrum (t = 0) to remove background noise and allow easier interpretation of results. To test activity with trione as substrate, 10 mM trione was used instead of 10 mM glucosone.

Half-life of BPP

The synthesis and $t_{1/2}$ of BPP was determined spectroscopically at 265 nm. The synthesis of BPP with D_1*D_2D_3 sonicate and 10 mM glucosone in a 500 μL reaction was followed until the absorbance reached ∼1.4 (about 14 min). The reaction was then passed through a 3,000 MWCO Nanosep centrifugal filter (PALL Life Sciences) by centrifuging for 4 min at 14,000 × g and 200 μL of filtrate followed at A_{265} every 4 s. The decay of A_{265} was normalized to the highest and lowest measured values, with the highest A_{265} set to 1 and the lowest to 0. To determine whether the $t_{1/2}$ was 0^{th}, 1^{st}, or 2^{nd} order, the natural log of the data was plotted against time. After determining that the decay followed 1^{st}-order decay, $t_{1/2}$ was calculated using the Solver add-in for Microsoft Excel, minimizing the sum of squared differences between the measured and modeled data calculated using Equation 1.

$$Normalized\ Abs = 1 * 0.5^{t/t_{1/2}} \quad \text{(Equation 1)}$$

D_1 activity with BPP and APM

BPP was generated from glucosone as described for the $t_{1/2}$ measurements and APM was generated similarly using AF (Carbosynth Ltd). Briefly, reactions with D_1*D_2D_3 sonicate and glucosone/AF was tracked, and 500 μL of the reaction passed through a 3,000 MWCO Nanosep centrifugal device (PALL Life Sciences) by centrifuging at 14,000 × g for 4 min. Domain 1 activity was determined as described for AUDH variant characterizations by UV spectroscopy, except for the substrate being replaced by filtrate containing BPP or APM.

Trione upgrading and recovery

The reaction of trione to produce glycolate esters (GE) or GA and 3,4-dihydroxybutyric acid (DHB) was carried out in batch mode. Reactions were performed using trione solution produced as described above. Most reactions were carried out in NMR tubes (Wilmad Lab-Glass WG-1000) at 298 K with various concentrations of base catalysts, including $NaHCO_3$ (Sigma Aldrich), Tris Base (Fisher Scientific), Bis-Tris (Ultrapure, ≥98% Dry Basis Fisher Scientific), and piperazine (99% Extra Pure, Acros Organics). Aqueous reaction solutions were prepared by dissolving the base catalyst in ultrapure water (18 MΩ) or D_2O (99.95%, Fisher Scientific) to which trione solution was added to achieve the desired reactant and base concentrations.

Analysis of the reaction was performed using NMR spectroscopy (Bruker Ascend 500, 500 MHz ^{1}H resonance frequency). ^{1}HNMR was used to study the reaction at short times (c.a., 2 h), with ^{13}CNMR spectroscopy used to study the reaction at longer times, extending past 24 h. Product identification was performed using ^{1}H-^{13}C HSQC NMR spectroscopy. Quantification by ^{13}CNMR spectroscopy was performed following progressive saturation[51] to identify scan parameters that lead to spectra collected at steady-state spin relaxation (4 s delay time, 1,024 scans, and 45° pulse width). The ^{13}CNMR shifts are reported relative to acetonitrile while the ^{1}HNMR shifts are reported relative to sodium trimethylsilylpropanesulfonate (DSS). Initial trione concentrations were verified by measuring a trione sample in the absence of base catalyst. Rates were calculated from *operando* ^{1}H and ^{13}CNMR experiments based on changes in reactant and product concentrations over the region where the concentration-vs.-time profile was approximately linear (corresponding to less than ca. 15% trione conversion).

Lactonization of DHB to HBL was performed in a 10 mL stirred glass batch reaction vials (Alltech) using HCl (38%, J.T. Baker) at pH 0.7 based on prior literature.[8] Quantification of total HBL was performed by HPLC (Waters ACQUITY UPC, equipped with a refractive index detector). Separation was achieved using an Aminex HPX-87H column with 5 mM aqueous H_2SO_4 as the mobile phase. Ethanol was used as an internal standard. Verification

of the chirality of the HBL was performed using gas chromatography flame ionization detection (GC-FID) using a chiral MilliporeSigma Supelco ß-Dex 225 Capillary GC column with helium carrier gas (inlet temperature, 250°C; column temperature, 205°C; FID temperature, 300°C; and carrier flow of 1 mL/min).

Liquid-liquid extraction of HBL from the product solution was performed in 10 mL stirred glass batch reaction vials (Alltech) followed by phase separation using a separatory funnel. Ethyl acetate (Acros Organics), propylene carbonate (Acros Organics), and tetrahydrofuran (Fisher) were evaluated as extraction solvents. Two-phase mixtures were allowed to rest for 24 h prior to phase separation. HBL was quantified in the aqueous and organic phases using GC-FID.

PA calculations

The PA for the homogeneous base catalysts was estimated from ground state DFT calculations, performed using Gaussian 16.[31] The Becke exchange functional and Lee-Yang-Parr correlation functional (B3LYP) were used in conjunction with a polarization diffuse function basis set (6-311+G). The PA was estimated as the difference between the total energies of the protonated and neutral forms of the homogeneous bases. In all cases, we considered the addition of a proton to the amine N of the piperazine and tris base while adding a proton to an O atom of sodium bicarbonate and bis-tris base.

RESOURCE AVAILABILITY

Lead contact

Requests for further information and resources should be directed to and will be fulfilled by the lead contact, Prof. Thomas J. Schwartz (thomas.schwartz@maine.edu).

Materials availability

The wild-type AUDH gene sequence (GenBank accession number KF699142), upon which variants are described here, was previously deposited. No other unique reagents were generated.

Data and code availability

The data that support the findings of this study are either available within the paper and supporting information or are available from the lead contact upon reasonable request. This paper does not report original code. Any additional information required to reanalyze the data reported in this paper is available from the lead contact upon request.

ACKNOWLEDGMENTS

At Forest Products Laboratory, we gratefully acknowledge Kolby C. Hirth for the NMR data collection for biological materials. At the University of Maine, we gratefully acknowledge Nick Hill for assistance with experimental setup, Dr. David Labrecque for assistance with NMR data collection, and Profs. Brian G. Frederick and M. Clayton Wheeler for helpful discussions. At the University of Wisconsin, we gratefully acknowledge Dr. Charles G. Fry for helpful discussions about NMR methods. Funding for this work was provided by the United States Department of Agriculture, US Forest Service Joint Ventures 18-JV-11111126-044 (to P.J.K. and J.A.D.) and 18-JV-11111126-045 (to P.J.K. and T.J.S), National Science Foundation grant OIA-233363 (to T.J.S.), and National Science Foundation grant CHE-1828408 (to T.J.S.).

AUTHOR CONTRIBUTIONS

Conceptualization, J.A.D., P.J.K., and T.J.S.; methodology, J.O.P.W., E.J., H.T.A., N.K., S.R.G., J.A.D., P.J.K., and T.J.S.; investigation, J.O.P.W., E.J., H.T.A., and N.K.; visualization, P.J.K. and T.J.S.; funding acquisition, J.A.D., P.J.K., and T.J.S.; project administration, J.A.D., P.J.K., and T.J.S.; supervision, S.R.G., J.A.D., P.J.K., and T.J.S.; Writing–original draft, J.O.P.W., E.J., H.T.A., S.R.G., P.J.K., and T.J.S.; writing–review & editing, S.R.G., J.A.D., P.J.K., and T.J.S. P.J.K. led and supervised the enzyme catalysis work, and T.J.S. led and supervised the acid/base catalysis work.

DECLARATION OF INTERESTS

The authors declare that US Patent Application 18/913,632 has been filed on the subject of this work.

SUPPLEMENTAL INFORMATION

Supplemental information can be found online at https://doi.org/10.1016/j.chempr.2025.102665.

Received: November 26, 2024
Revised: April 4, 2025
Accepted: June 24, 2025

REFERENCES

1. Aitken, M., Kleinrock, M., and Munoz, E. (2021). Global Medicine Spending And Usage Trends: Outlook To 2025. IQVIA. https://www.iqvia.com/insights/the-iqvia-institute/reports/global-medicine-spending-and-usage-trends-outlook-to-2025.
2. Langreth, R. (2023) Why Prescription Drug Prices in the US Are so High. Published Online July 19, 2022.
3. Lapham, L.H. (2009) The God in the Machine. Lapham's Quarterly *2*.
4. (2022). Chiral Building Blocks in Asymmetric Synthesis (Wiley-VCH Verlag).
5. Andrushko, V., and Andrushko, N. (2013). Stereoselective Synthesis of Drugs and Natural Products (John Wiley & Sons, Incorporated).
6. Bozell, J.J., and Petersen, G.R. (2010). Technology development for the production of biobased products from biorefinery carbohydrates—the US Department of Energy's "Top 10" revisited. Green Chem. *12*, 539–554. https://doi.org/10.1039/b922014c.
7. Werpy, T., and Peterson, G. (2004) Top Value Added Chemicals from Biomass: Volume I—Results of Screening for Potential Candidates from Sugars Ans Synthesis Gas. DOE/GO-102004-101992. U.S. Department of Energy. https://www.nrel.gov/docs/fy04osti/35523.pdf.
8. Martin, C.H., Dhamankar, H., Tseng, H.-C., Sheppard, M.J., Reisch, C.R., and Prather, K.L.J. (2013). A platform pathway for production of 3-hydroxyacids provides a biosynthetic route to 3-hydroxy-g-butyrolactone. Nat. Commun. *4*, 1414. https://doi.org/10.1038/ncomms2418.
9. Lee, S.-H., and Park, O.-J. (2009). Uses and production of chiral 3-hydroxy-g-butyrolactones and structurally related chemicals. Appl. Microbiol. Biotechnol. *84*, 817–828. https://doi.org/10.1007/s00253-009-2143-0.
10. Saito, S., Hasegawa, T., Inaba, M., Nishida, R., Fujii, T., Nomizu, S., and Moriwake, T. (1984). Combination of borane-dimethyl sulfide complex with catalytic sodium tetrahydroborate as a selective reducing agent for α-hydroxy esters. Versatile chiral building block from (S)-(−)-malic acid. Chem. Lett. *13*, 1389–1392. https://doi.org/10.1246/cl.1984.1389.
11. Hollingsworth, R.I. (1998). Process for the preparation of hydroxy substituted gamma butyrolactones. US Patent USRE38324E1.
12. Dhamankar, H., Tarasova, Y., Martin, C.H., and Prather, K.L.J. (2014). Engineering E. coli for the biosynthesis of 3-hydroxy-γ-butyrolactone (3HBL) and 3,4-dihydroxybutyric acid (3,4-DHBA) as value-added chemicals from glucose as a sole carbon source. Metab. Eng. *25*, 72–81. https://doi.org/10.1016/j.ymben.2014.06.004.
13. Cao, Y., Niu, W., Guo, J., Guo, J., Liu, H., Liu, H., and Xian, M. (2023). Production of Optically Pure (S)-3-Hydroxy-γ-butyrolactone from d-Xylose

Using Engineered Escherichia coli. J. Agric. Food Chem. *71*, 20167–20176. https://doi.org/10.1021/acs.jafc.3c06589.

14. Schwartz, T.J., O'Neill, B.J., Shanks, B.H., and Dumesic, J.A. (2014). Bridging the chemical and biological catalysis gap: Challenges and outlooks for producing sustainable chemicals. ACS Cat. *4*, 2060–2069. https://doi.org/10.1021/cs500364y.
15. Schwartz, T.J., Shanks, B.H., and Dumesic, J.A. (2016). Coupling chemical and biological catalysis: A flexible paradigm for producing biobased chemicals. Curr. Opin. Biotechnol. *38*, 54–62. https://doi.org/10.1016/j.copbio.2015.12.017.
16. Schwartz, T.J., Goodman, S.M., Osmundsen, C.M., Taarning, E., Mozuch, M.D., Gaskell, J., Cullen, D., Kersten, P.J., and Dumesic, J.A. (2013). Integration of chemical and biological catalysis: Production of furylglycolic acid from glucose via cortalcerone. ACS Cat. *3*, 2689–2693. https://doi.org/10.1021/cs400593p.
17. Baute, M.A., Baute, R., Deffieux, G., and Filleau, M.J. (1977). Conversion of glucose to cortalcerone via glucosone by *Corticium Caeruleum*. Phytochemistry *16*, 1895–1897. https://doi.org/10.1016/0031-9422(77)80091-5.
18. Koths, K., Halenbeck, R., and Moreland, M. (1992). Synthesis of the antibiotic cortalcerone from D-glucose using pyranose 2-oxidase and a novel fungal enzyme, aldos-2-ulose dehydratase. Carbohydr. Res. *232*, 59–75. https://doi.org/10.1016/s0008-6215(00)90994-7.
19. de Koker, T.H., Mozuch, M.D., Cullen, D., Gaskell, J., and Kersten, P.J. (2004). Isolation and purification of pyransoe 2-oxidase from *Phanerochaete chrysoporium* and characterization of gene structure and regulation. Appl. Environ. Microbiol. *70*, 5794–5800. https://doi.org/10.1128/AEM.70.10.5794-5800.2004.
20. Daniel, G., Volc, J., and Kubatova, E. (1994). Pyranose oxidase, a major source of H_2O_2 during wood degradation by *Phanerochaete chrysosporium*, *Trametes versicolor*, and *Oudemansiella mucida*. Appl. Environ. Microbiol. *60*, 2524–2532. https://doi.org/10.1128/aem.60.7.2524-2532.1994.
21. Volc, J., Kubátová, E., Daniel, G., and Přikrylová, V. (1996). Only C-2 specific glucose oxidase activity is expressed in ligninolytic cultures of the white rot fungus *Phanerochaete chrysosporium*. Arch. Microbiol. *165*, 421–424. https://doi.org/10.1007/s002030050348.
22. Abrera, A.T., Sützl, L., and Haltrich, D. (2020). Pyranose oxidase: A versatile sugar oxidoreductase for bioelectrochemical applications. Bioelectrochemistry *132*, 107409. https://doi.org/10.1016/j.bioelechem.2019.107409.
23. Giffhorn, F. (2000). Fungal pyranose oxidases: Occurrence, properties and biotechnical applications in carbohydrate chemistry. Appl. Microbiol. Biotechnol. *54*, 727–740. https://doi.org/10.1007/s002530000446.
24. Hori, C., Ishida, T., Igarashi, K., Samejima, M., Suzuki, H., Master, E., Ferreira, P., Ruiz-Dueñas, F.J., Held, B., Canessa, P., et al. (2014). Analysis of the *Phlebiopsis gigantea* genome, transcriptome and secretome provides insight into its pioneer colonization strategies of wood. PLOS Genet. *10*, e1004759. https://doi.org/10.1371/journal.pgen.1004759.
25. Mozuch, M.D., Hirth, K.C., Schwartz, T.J., and Kersten, P.J. (2021). Repurposing inflatable packaging pillows as bioreactors: a convenient synthesis of glucosone by whole-cell catalysis under oxygen. Appl. Biochem. Biotechnol. *193*, 743–760. https://doi.org/10.1007/s12010-020-03448-x.
26. Claesson, M., Lindqvist, Y., Madrid, S., Sandalova, T., Fiskesund, R., Yu, S., and Schneider, G. (2012). Crystal structure of bifunctional aldos-2-ulose dehydratase/Isomerase from *Phanerochaete chrysosporium* with the reaction intermediate ascopyrone M. Journal. J. Mol. Biol. *417*, 279–293. https://doi.org/10.1016/j.jmb.2012.02.001.
27. Yu, S. (2005). Enzymatic description of the anhydrofructose pathway of glycogen degradation – II. Gene identification and characterization of the reactions catalyzed by aldos-2-ulose dehydratase that converts 1,5-anhydro-D-fructose to microthecin with ascopyrone M as the intermediate. Biochim. Biophys. Acta *1723*, 63–73. https://doi.org/10.1016/j.bbagen.2005.01.004.
28. Baute, M.-A., Deffieux, G., Vercauteren, J., Baute, R., and Badoc, A. (1993). Enzymic activity degrading 1,4-a-D-glucans to ascopyrones P and T in *Pezizales* and *Tuberales*. Phytochemistry *33*, 41–45. https://doi.org/10.1016/0031-9422(93)85393-6.
29. Yu, S., Andreassen, M., and Lundt, I. (2008). Enzymatic production of microthecin by aldos-2-ulose dehydratase from 1,5-anhydro-D-fructose and stability studies of microthecin. Biocatal. Biotransform. *26*, 169–176. https://doi.org/10.1080/10242420701799477.
30. Anslyn, E.V., and Dougherty, D.A. (2006). Modern Physical Organic Chemistry, Third Edition (University Science Books).
31. Frisch, M.J., Trucks, G.W., Schlegel, H.B., Scuseria, G.E., Robb, M.A., Cheeseman, J.R., Scalmani, G., Barone, V., Petersson, G.A., Nakatsuji, H., et al. (2016). Gaussian 16. Rev. C *01*.
32. Carey, F.A. (2000). Organic Chemistry, Fourth Edition (McGraw Hill).
33. Lewis, J.D., Van de Vyver, S., and Román-Leshkov, Y. (2015). Acid–Base Pairs in Lewis Acidic Zeolites Promote Direct Aldol Reactions by Soft Enolization. Angew. Chem. Int. Ed. Engl. *54*, 9835–9838. https://doi.org/10.1002/anie.201502939.
34. Cañada-Barcala, A., Rodríguez-Llorente, D., López, L., Navarro, P., Hernández, E., Águeda, V.I., Álvarez-Torrellas, S., Parajó, J.C., Rivas, S., and Larriba, M. (2021). Sustainable Production of Furfural in Biphasic Reactors Using Terpenoids and Hydrophobic Eutectic Solvents. ACS Sustainable Chem. Eng. *9*, 10266–10275. https://doi.org/10.1021/acssuschemeng.1c02798.
35. Lee, S.-H., Park, O.-J., and Uh, H.-S. (2008). A chemoenzymatic approach to the synthesis of enantiomerically pure (S)-3-hydroxy-g-butyrolactone. Appl. Microbiol. Biotechnol. *79*, 355–362. https://doi.org/10.1007/s00253-008-1439-9.
36. Turton, R., Bailie, R.C., Whiting, W.B., and Shaeiwitz, J.A. (2009). Analysis, Synthesis, and Design of Chemical Processes, Third Edition (Prentice Hall).
37. Rouhi, A.M. (2003). Custom Chemicals. Chem. Eng. News Archive *81*, 55–73. https://doi.org/10.1021/cen-v081n007.p055.
38. Plus, A. (2019) (AspenTech).
39. Clippinger, J., and Davis, R. (2019). Techno-Economic Analysis for the Production of Algal Biomass via Closed Photobioreactors: Future Cost Potential Evaluated Across a Range of Cultivation System Designs (National Renewable Energy Laboratory. National Renewable Energy Laboratory, Office of Energy Efficiency and Renewable Energy). TP-5100-72716. https://www.nrel.gov/docs/fy19osti/72716.pdf.
40. Humbird, D., Davis, R., Tao, L., Kinchin, C., Hsu, D., Aden, A., Schoen, P., Lukas, J., Olthof, B., Worley, M., et al. (2011). Process Design and Economics for Biochemical Conversion of Lignocellulosic Biomass to Ethanol (National Renewable Energy Laboratory. National Renewable Energy Laboratory, Office of Energy Efficiency and Renewable Energy). TP-5100-47764. https://www.nrel.gov/docs/fy11osti/47764.pdf.
41. Mofarahi, M., and Seyyedi, M. (2009). Pure and Binary Adsorption Isotherms of Nitrogen and Oxygen on Zeolite 5A. J. Chem. Eng. Data *54*, 916–921. https://doi.org/10.1021/je8006919.
42. Zhou, X., Zha, M., Cao, J., Yan, H., Feng, X., Chen, D., and Yang, C. (2021). Glycolic Acid Production from Ethylene Glycol via Sustainable Biomass Energy: Integrated Conceptual Process Design and Comparative Techno-economic–Society–Environment Analysis. ACS Sustainable Chem. Eng. *9*, 10948–10962. https://doi.org/10.1021/acssuschemeng.1c03717.
43. Datta, R. (2000). Hydroxycarboxylic Acids. In Kirk-Othmer Encyclopedia of Chemical Technology (John Wiley & Sons, Inc.). https://doi.org/10.1002/0471238961.0825041804012020.a01.pub2.
44. Yi, Y.-C., and Ng, I.-S. (2023). Toward Low-Carbon-Footprint Glycolic Acid Production for Bioplastics through Metabolic Engineering in *Escherichia coli*. ACS Sustainable Chem. Eng. *11*, 815–823. https://doi.org/10.1021/acssuschemeng.2c06718.

45. Schwartz, T.J., and Lawoko, M. (2010). Removal of acid-soluble lignin from biomass extracts using Amberlite XAD-4 resin. BioResources *5*, 2337–2347. https://doi.org/10.15376/biores.5.4.2337-2347.

46. Deng, Y., Ma, N., Zhu, K., Mao, Y., Wei, X., and Zhao, Y. (2018). Balancing the carbon flux distributions between the TCA cycle and glyoxylate shunt to produce glycolate at high yield and titer in *Escherichia coli*. Metab. Eng. *46*, 28–34. https://doi.org/10.1016/j.ymben.2018.02.008.

47. Bhagwat, S.S., Li, Y., Cortés-Peña, Y.R., Brace, E.C., Martin, T.A., Zhao, H., and Guest, J.S. (2021). Sustainable Production of Acrylic Acid via 3-Hydroxypropionic Acid from Lignocellulosic Biomass. ACS Sustainable Chem. Eng. *9*, 16659–16669. https://doi.org/10.1021/acssuschemeng.1c05441.

48. Pisanelli, I., Kujawa, M., Spadiut, O., Kittl, R., Halada, P., Volc, J., Mozuch, M.D., Kersten, P., Haltrich, D., and Peterbauer, C. (2009). Pyranose oxidase from *Phanerochaete chrysosporium* – expressin in *E. coli* and biochemical characterization. J. Biotechnol. *142*, 97–106. https://doi.org/10.1016/j.jbiotec.2009.03.019.

49. Studier, F.W. (2005). Protein production by auto-induction in high-density shaking cultures. Protein Expr. Purif. *41*, 207–234. https://doi.org/10.1016/j.pep.2005.01.016.

50. Blommel, P.G., and Fox, B.G. (2007). A combined approach to improving large-scale production of tobacco etch virus protease. Protein Expr. Purif. *55*, 53–68. https://doi.org/10.1016/j.pep.2007.04.013.

51. Freeman, R., and Hill, H.D.W. (1971). Fourier Transform Study of NMR Spin–Lattice Relaxation by "Progressive Saturation". J. Chem. Phys. *54*, 3367–3377. https://doi.org/10.1063/1.1675352.